The Short-Range Structure around Li^+ in Highly Concentrated Aqueous LiBr Solutions

Yasuo Kameda,* Shun Suzuki, Hidekazu Ebata, Takeshi Usuki, and Osamu Uemura

Department of Material and Biological Chemistry, Faculty of Science, Yamagata University, Kojirakawa-machi 1-4-12, Yamagata 990

(Received June 10, 1996)

Neutron diffraction measurements have been carried out on aqueous 10, 25, and 33 mol% LiBr solutions. The $^6Li/^7Li$ isotopic substitution technique was applied to determine the local structure around Li^+ in these solutions. The least-squares fitting analysis was successfully adopted both for the observed Li^+ difference interference function, $\Delta_{Li}(Q)$, and for the Li^+ distribution function $G_{Li}(r)$. The nearest neighbor $Li^+\cdots O$ distance in the solutions was obtained to be 1.96±0.02 Å, which agrees well with that reported in previous neutron diffraction studies. The average hydration number of Li^+ decreases from ca. 6 for the 10 mol% LiBr solution to ca. 4 for the 25 mol% LiBr solution. The tetrahedral hydration structure around Li^+ appeared to stay even in the 33 mol% LiBr solution. The $Li^+\cdots Br^-$ correlation was found at 3.4 Å in the 33 mol% LiBr solution. This value rather suggests the formation of the solvent-shared ion pair, $Li^+\cdots D_2O\cdots Br^-$.

In highly concentrated aqueous solutions containing considerable amounts of solute ions as compared with solvent water molecules, not only the hydrogen-bond interaction between water molecules but also the electrostatic interaction among solute ions plays an important role for various properties of the solution. Studies on the microscopic structures in aqueous lithium halogenide (LiX) solutions are one of the most useful means of investigating these interactions in highly concentrated aqueous solutions because of the very high solubility of LiX to water.

The hydration structure of Li^+ in aqueous solutions has been investigated variously by X-ray[1—10] and neutron[4,7,8,11—24] diffraction techniques and by molecular dynamics (MD) simulations.[6—9] Nevertheless, there still remain unsolved problems, particularly in the high concentration range, concerning the $Li^+\cdots O$ distance, $Li^+\cdots X^-$ contact ion pair formation and hydration structure of Li^+. The nearest-neighbor $Li^+\cdots O$ distance obtained by X-ray diffraction studies is 0.1—0.2 Å larger than that determined by neutron diffraction studies beyond experimental uncertainties. This inconsistency may mainly arise from the difference in the scattering mechanism between the two diffractions;[25] i.e., incident neutrons are scattered by atomic nuclei in the sample, while X-ray photons are scattered by electron clouds belonging to atoms which are significantly deformed from the spherical distribution by polarization and/or chemical bonding effects. Another cause may be that the $Li^+\cdots O$ distance is affected by the hydration geometry around Li^+, as pointed out by Ohtaki and Radnai.[25] The strong concentration dependence of the hydration number of Li^+ has been observed in neutron diffraction[12,15,24] and MD[7—9] studies. On the contrary, according to the neutron diffraction studies employing the first order difference method[26,27] the $Li^+\cdots O$ distance remains roughly unchanged in solutions with various solute concentrations.[12,13,15—24]

The formation of $Li^+\cdots X^-$ contact ion pairs in aqueous lithium halogenide solutions has been reported only in the highly concentrated LiCl solution by neutron diffraction (33 mol% LiCl),[15] and X-ray diffraction (25 mol% LiCl)[9] studies. According to Ichikawa et al., each Li^+ is surrounded by 2.3 water molecules and 1.5 chloride ions[15] in the 33 mol% LiCl solution, leading to a tetrahedral coordination geometry of Li^+. Copestake et al. have proposed from the results of partial pair distribution function, $g_{ClCl}(r)$, experimentally obtained, that Li^+ is simultaneously bonded to 3 chloride ions in the 23 mol% LiCl solution, under the assumption of the octahedral coordination geometry of Li^+.[28] On the other hand, recent Raman spectroscopic studies have shown that the symmetric stretching vibrational mode of the $Li^+X^-(H_2O)_n$ complex appears around 370 and 340 cm^{-1} in both 25 mol% LiCl and LiBr solutions.[29,30] Intermolecular hydrogen-bonded structure in concentrated aqueous LiCl and LiBr solutions have been investigated by H/D isotopic substitution technique combined with the neutron diffraction.[21,31—33] Clear evidence for deformation of the hydrogen-bonds among the solvent water molecules was obtained in the concentrated solutions above ca. 15 mol% LiX. Consequently, further structural investigations are needed to solve these inconsistencies in highly concentrated LiX solutions.

In this paper, we describe results of neutron diffraction measurements on aqueous 10, 25, and 33 mol% LiBr solutions, in which the isotopic ratio of $^6Li/^7Li$ is changed. The concentration dependence of the hydration geometry around Li^+ is discussed using the distribution function around Li^+, $G_{Li}(r)$, obtained by the first-order difference method. The

Table 1. The Isotopic Compositions, Mean Scattering Lengths b_{Li} for Lithium Atom, Mean Scattering and Absorption Cross Sections and the Number Density Scaled in the Stoichiometric Unit $(LiBr)_x(D_2O)_{1-x}$, σ_s, σ_a, and ρ_0, Respectively, for Sample Solutions Used in This Study

Samples	^{6}Li/%	^{7}Li/%	$b_{Li}/10^{-12}$ cm[a]	σ_s/ barns[b]	σ_a/ barns[c]	$\rho_0/Å^{-3}$
$(^6LiBr)_{0.10}(D_2O)_{0.90}$	95.4	4.6	0.181	11.82	50.20	0.0317
$(^7LiBr)_{0.10}(D_2O)_{0.90}$	0.1	99.9	−0.222	11.85	0.42	
$(^0LiBr)_{0.25}(D_2O)_{0.75}$[d]	54.1	45.9	0.006	11.04	71.46	0.0298
$(^7LiBr)_{0.25}(D_2O)_{0.75}$	0.1	99.9	−0.222	11.10	1.05	
$(^0LiBr)_{0.33}(D_2O)_{0.67}$	54.1	45.9	0.006	8.76	96.17	0.0279
$(^{nat}LiBr)_{0.33}(D_2O)_{0.67}$[e]	7.5	92.5	−0.190	8.84	16.04	

a) Taken from Ref. 34. b) Calculated using total cross sections for liquid D_2O.[35,36] c) For incident neutron wavelength of 1.008 Å. d) The superscript "0" denotes an isotopic mixture $b_{Li}=0$. e) The superscript "nat" denotes the natural abundance.

least squares fit analysis is also applied to the Li^+ difference interference function, $\Delta_{Li}(Q)$, in order to confirm whether the result deduced from $G_{Li}(r)$ is reasonable.

Experimental and Data Analysis

Materials. ^{6}Li- and ^{7}Li-enriched lithium bromides were respectively prepared by reacting $^6Li_2CO_3$ (95.45% ^{6}Li) and $^7LiOH\cdot H_2O$ (99.94% ^{7}Li, Tomiyama Chemical Co., Ltd.), with slightly excess amounts of the concentrated aqueous hydrobromic acid solution (Nacalai Tesque, Guaranteed grade). The product solution was dehydrated by heating at 180 °C for two days under the vacuum. Weighed amounts of enriched anhydrous LiBr were dissolved into D_2O (99.9% D, Aldrich Chemical Inc., Co.) to prepare aqueous 10, 25, and 33 mol% LiBr solutions with different Li isotopic compositions. The sample solution was sealed into a cylindrical quartz cell (11.4 mm in inner diameter and 1.2 mm in thickness). Sample parameters are listed in Table 1. The coherent scattering length, b, as well as the scattering and absorption cross sections, σ_s and σ_a, for the nuclei, Li, Br, and O, were respectively referred to based on those tabulated by Sears.[34] Scattering cross sections for H and D nuclei within the water molecules, $\sigma_{s,H}=33.55$ barns and $\sigma_{s,D}=4.04$ barns, which were calculated from the observed total cross sections for liquid H_2O and D_2O,[35,36] were employed for both the absorption and multiple scattering corrections in this work. In order to reduce uncertainties arising from the large neutron-absorption ability of ^{6}Li, the isotopic composition of the "null mixture", in which the mean scattering length of Li is zero, was employed for both 25 and 33 mol% LiBr solutions.

Neutron Diffraction Measurements. Neutron diffraction measurements were carried out using the ISSP diffractometer (PANSI) at the JRR-2 research reactor operated at 10 MW in Japan Atomic Energy Research Institute, Tokai-mura, Japan. The incident neutron wavelength, $\lambda=1.008\pm0.003$ Å, was determined by Bragg reflections from KCl powder. Collimations used were 40′–40′ in going from the reactor to the detector. The aperture of the collimated beam was 20 mm in width and 40 mm in height. Diffraction measurements were carried out at 25 °C, 100 °C and 130 °C for 10, 25, and 33 mol% LiBr solutions in D_2O, respectively. The temperature of the sample was monitored with a Cromel–Almel thermocouple and controlled within ± 3 °C. Scattered neutrons from the sample were collected over the angular range of $3\leq 2\theta\leq 102°$, which corresponds to $0.32\leq Q\leq 9.69$ Å^{-1} (the scattering vector magnitude $Q=4\pi\sin\theta/\lambda$). The step interval was chosen to be $\Delta(2\theta)=0.5°$ in the range of $3\leq 2\theta\leq 40°$ and $\Delta(2\theta)=1°$ in the range of $41\leq 2\theta\leq 102°$, respectively. The preset time was 240—300 s for the 10 and 25 mol% LiBr solutions and 450—500 s for the 33 mol% LiBr solution. Scattering intensities were measured in advance for a vanadium rod (10 mm in diameter), empty cell and background, respectively. Measured scattering intensities were corrected for the background, absorption of both the sample and cell[37] and multiple scattering intensities.[38] The obtained count rate for the sample was converted to the absolute scale by the use of scattering intensities from the vanadium rod. Details of the data correction and normalization procedure have already been described in our previous paper.[21]

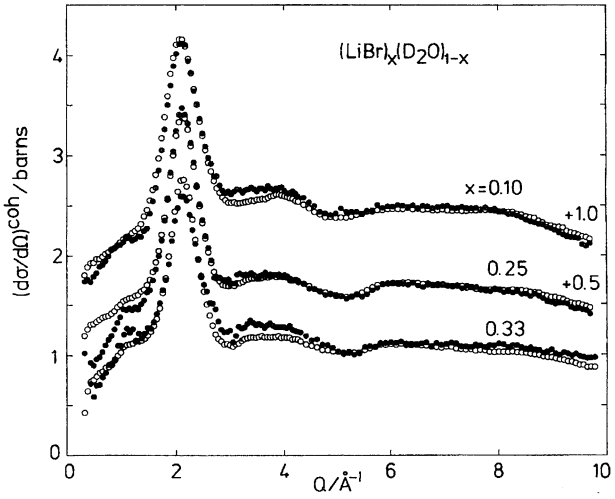

Fig. 1. Observed scattering cross sections $(d\sigma/d\Omega)^{coh}$ for aqueous LiBr solutions, $(LiBr)_x(D_2O)_{1-x}$, $x=0.10$, 0.25, and 0.33, with different isotope ratio of ^{6}Li/^{7}Li. Full circles denote data points for sample solutions with higher ^{6}Li content.

Results and Discussion

Observed scattering cross sections, $(d\sigma/d\Omega)^{coh}$, for aqueous 10, 25, and 33 mol% LiBr solutions in D_2O are shown in Fig. 1. The overall features of $(d\sigma/d\Omega)^{coh}$ with different ^{6}Li/^{7}Li ratios look very similar at the corresponding solute compositions. However, a systematic difference in the intensity of $(d\sigma/d\Omega)^{coh}$ can be observed around $Q=1.1$ and 3—4 Å^{-1}, respectively, according to the difference in the scattering length of the Li nuclei. A gradual fall in the intensity of $(d\sigma/d\Omega)^{coh}$ at the larger Q side is mainly due to the inelas-

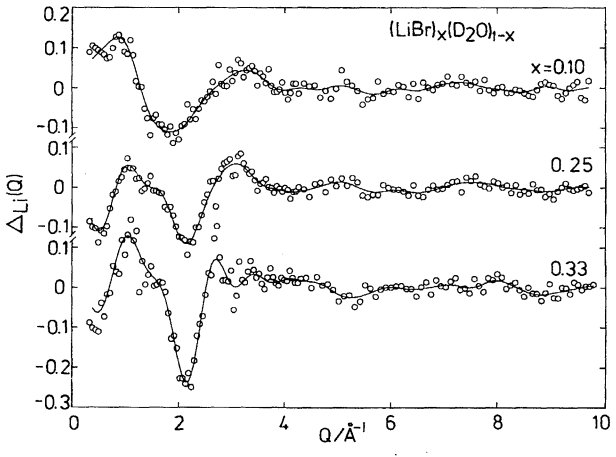

Fig. 2. Observed difference function $\Delta_{Li}(Q)$ for aqueous LiBr solutions, $(LiBr)_x(D_2O)_{1-x}$, $x=0.10$, 0.25, and 0.33 (circles). Solid lines are given by the inverse Fourier transform of the observed $G_{Li}(r)$ in Fig. 3 in which unphysical ripples below the first peak have been corrected.

ticity effect of deuterium atoms in solvent molecules, which is roughly proportional to $\sin^2\theta$.[39,40] In order to elucidating the environmental structure around Li^+, the first-order difference interference function,[26,27] $\Delta_{Li}(Q)$, was evaluated by the numerical difference in $(d\sigma/d\Omega)^{coh}$ between the same LiBr concentration solutions with different Li isotopic compositions, as seen in Fig. 2. The main advantage of the first-order difference method is the cancellation of the inelasticity distortion between individual intensity curves. The difference interference function scaled by a stoichiometric unit, $(LiBr)_x(D_2O)_{1-x}$, $\Delta_{Li}(Q)$, between two solutions which are identical in all respects except for different isotopic states of Li, can be expressed as the weighted sum of four partial structure factors;

$$\Delta_{Li}(Q)=A[a_{LiO}(Q)-1]+B[a_{LiD}(Q)-1]+C[a_{LiBr}(Q)-1] +D[a_{LiLi}(Q)-1]+\text{the correction term}, \quad (1)$$

and

$$A=2x(1-x)b_O(b_{Li}-b'_{Li}),\ B=4x(1-x)b_D(b_{Li}-b'_{Li}),$$
$$C=2x(1-x)b_{Br}(b_{Li}-b'_{Li}),\ D=x^2({b_{Li}}^2-{b'_{Li}}^2),$$

where b_i stands for the mean scattering length of nucleus i. Contributions from atomic pairs which do not include Li^+ are completely canceled out in $\Delta_{Li}(Q)$. The correction term in Eq. 1 results from a slight difference in the inelasticity contribution in the self intensity term between ^6Li and ^7Li, which is negligibly small.[13,26] Coefficients of respective partial structure factors in $\Delta_{Li}(Q)$ are listed up in Table 2. In the calculation, the following values were used for the coherent scattering lengths:[34] $b_O=0.5805$, $b_D=0.6653$, and $b_{Br}=0.679$. The Fourier transform of $\Delta_{Li}(Q)$ gives the environmental distribution function around Li^+, $G_{Li}(r)$, as shown in Fig. 3. $G_{Li}(r)$ is related to the weighted sum of partial distribution functions as follows:

Table 2. Values of the Coefficients of $a_{ij}(Q)$ in Eq. 1

Samples	A/barns	B/barns	C/barns	D/barns
$(^*LiBr)_{0.10}(D_2O)_{0.90}$	0.0421	0.0965	0.0055	−0.0002
$(^*LiBr)_{0.25}(D_2O)_{0.75}$	0.0496	0.1138	0.0194	−0.0031
$(^*LiBr)_{0.33}(D_2O)_{0.67}$	0.0503	0.1153	0.0290	−0.0039

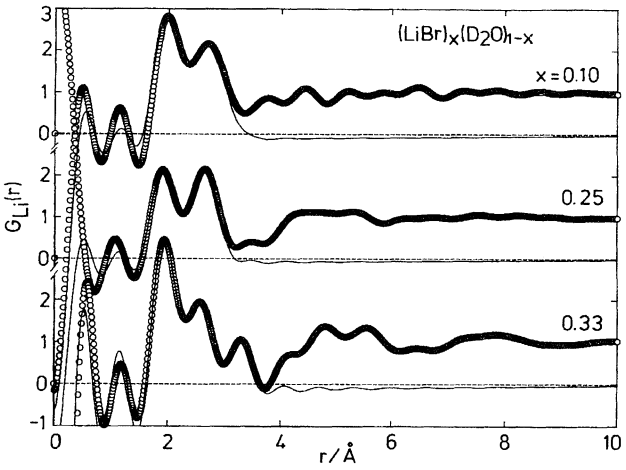

Fig. 3. The distribution function around Li^+ for aqueous LiBr solutions, $(LiBr)_x(D_2O)_{1-x}$, x=0.10, 0.25, and 0.33 (circles). Solid lines are given by the Fourier transform of the theoretical interference term, $i^{calc}(Q)$, (Eq. 3) for the nearest neighbor $Li^+\cdots j$ pairs.

$$G_{Li}(r)=1+(A+B+C+D)^{-1}(2\pi^2\rho r)^{-1}\int_0^{Q_{max}} Q\Delta_{Li}(Q)\sin(Qr)dQ$$
$$=[Ag_{LiO}(r)+Bg_{LiD}(r)+Cg_{LiBr}(r)+Dg_{LiLi}(r)](A+B+C+D)^{-1}, \quad (2)$$

where ρ is the number density of atoms in the stoichiometric unit $(LiBr)_x(D_2O)_{1-x}$. The upper limit, Q_{max}, in the Fourier integral was taken to be 9.69 $Å^{-1}$ for all $G_{Li}(r)$ in the present work. The truncation effect due to the limited Q_{max} causes serious ripples in $G_{Li}(r)$, particularity in the small r region. In order to check the self-consistency between $\Delta_{Li}(Q)$ and $G_{Li}(r)$, unphysical oscillations below the first peak in $G_{Li}(r)$ were eliminated by setting the function values null. $G_{Li}(r)$ was then back Fourier-transformed to obtain the corrected $\Delta_{Li}(Q)$ as indicated by the solid line in Fig. 2. The corrected $\Delta_{Li}(Q)$ agrees well with the observed one within statistical uncertainties, that is to say, unphysical ripples below the first peak in $G_{Li}(r)$ appeared to arise substantially from the truncation effect. The present $G_{Li}(r)$ has a similar functional form to that already shown in previous works,[12—24] i.e., well-resolved Li–O and Li–D peaks which indicate the presence of distinct first hydration shell of Li^+ with a settled orientation between Li^+ and the neighboring water molecules. As new structural information, it can be emphasized that the present $G_{Li}(r)$ has a peak at $r\approx3.3$ Å in the 33 mol% LiBr solution, in which there are only two water molecules per one Li^+. Then we assign this peak to the nearest neighbor $Li^+\cdots Br^-$ correlation. In addition, a broadened peak, perhaps belonging to the second hydration shell, can be observed at r=4—6

Å in $G_{Li}(r)$ in both 25 and 33 mol% LiBr solutions.

In order to evaluate structural parameters relating to the first coordination shell of Li^+ using the truncated $G_{Li}(r)$, we carry out the least-squares fit for $G_{Li}(r)$, according to the procedure described below.

i) the theoretical interference term, $i^{calc}(Q)$, consisting of the nearest neighbor $Li^+\cdots j$ pairs (j=O, D for 10 and 25 mol% LiBr and j=O, D, and Br for 33 mol% LiBr solution, respectively) is introduced as follows:

$$i^{calc}(Q)=\sum 2xn_{Lij}(b_{Li}-b'_{Li})b_j\exp(-l_{Lij}^2Q^2/2)\sin(Qr_{Lij})/(Qr_{Lij}), \quad (3)$$

where n_{Lij} denotes the coordination number of atom j around Li^+. l_{Lij} and r_{Lij} give the root mean square displacement and internuclear distance for the $Li^+\cdots j$ pair, respectively.

ii) $i^{calc}(Q)$ is converted to the theoretical distribution function, $G^{calc}(r)$, through the Fourier transform, i.e.,

$$G^{calc}(r)=(A+B+C+D)^{-1}(2\pi^2\rho r)^{-1}\int_0^{Q_{max}}Qi^{calc}(Q)\sin(Qr)dQ. \quad (4)$$

The upper limit of the integral is set to be the same value (9.69 $Å^{-1}$) already used for the derivation of $G_{Li}(r)$.

iii) Least-squares refinements of parameter values in Eq. 3, such as n_{Lij}, l_{Lij}, and r_{Lij}, are made through minimizing the integrated value U defined below,

$$U=\int_{r_1}^{r_2}[G_{Li}(r)-G^{calc}(r)]^2dr. \quad (5)$$

Lower and upper limits of the integral were chosen to be r_1=1.70 Å and r_2=3.00 Å for the 10 and 25 mol% LiBr solutions, and r_1=1.60 Å and r_2=3.72 Å for the 33 mol% LiBr solution, respectively. In the refinement, n_{LiD} was assumed to be twice the value of n_{LiO}, considering the ratio D/O=2/1 within one D_2O molecule. The contribution from the nearest neighbor $Li^+\cdots Br^-$ pair is involved only for the 33 mol% LiBr solution. The fitting procedure was performed using the SALS program.[41]

In Fig. 3, theoretical distribution functions $G^{calc}(r)$, (denoted by solid lines), given by the best fit of the first hydration model, are compared with the observed $G_{Li}(r)$. A satisfactory agreement is obtained between $G^{calc}(r)$ and $G_{Li}(r)$ in the range of $r_1\leq r\leq r_2$ which was covered in the fitting procedure. The values of independent parameters obtained are as follows: r_{LiO}=1.98(2) Å, l_{LiO}=0.19(2) Å, r_{LiD}=2.71(2) Å, l_{LiD}=0.30(2) Å, and n_{LiO}=6.5(5) for 10 mol% LiBr solution, r_{LiO}=1.94(2) Å, l_{LiO}=0.18(2) Å, r_{LiD}=2.65(2) Å, l_{LiD}=0.23(2) Å and n_{LiO}=4.2(5) for 25 mol% LiBr solution, r_{LiO}=1.94(2) Å, l_{LiO}=0.07(2) Å, r_{LiD}=2.51(2) Å, l_{LiD}=0.28(2) Å, n_{LiO}=3.7(2), r_{LiBr}=3.30(2) Å, l_{LiBr}=0.15(1) Å, and n_{LiBr}=3.5(5) for 33 mol% LiBr solution. The average hydration number of Li^+ decreases from ca. 6 at 10 mol% LiBr to ca. 4 at 25 mol% LiBr solution. The similar concentration dependence of n_{LiO} has been reported in recent neutron diffraction work for concentrated aqueous LiCl solutions by Howell and Neilson.[24] The hydration number 3.7 for the present 33 mol% LiBr solution may imply that the tetrahedral hydration structure around Li^+ is retained at such the high solute concentration. The present value of n_{LiO} for the 33 mol% LiBr solutions is considerably larger than that obtained for the 33 mol% LiCl solution, in which 2.3 water molecules and 1.5 chloride ions are in direct contact with Li^+.[15] The present value of the nearest neighbor $Li^+\cdots Br^-$ distance in the 33 mol% LiBr solution is ca. 0.5 Å larger than that reported in crystalline β-LiBr·H_2O (r_{LiBr}=2.84 Å),[42] in which Br^- is in direct contact with Li^+. It may be that Br^- does not directly contact with Li^+, and the solvent-shared ion pair, $Li^+\cdots D_2O\cdots Br^-$, is rather formed in the 33 mol% LiBr solution. It may be expected that Br^- lies in a dip formed by three water molecules which occupy corner sites in the hydration tetrahedron with Li^+ at the central site. The present value of r_{LiO} for the 25 and 33 mol% LiBr solutions (1.94(2) Å) is in reasonable agreement with that reported in previous works done with the neutron diffraction method.[11—24] A slightly larger value, r_{LiO}=1.98(2) Å, is obtained for the 10 mol% LiBr solution. An indication of the concentration-dependent hydration geometry of the nearest neighbor water molecules around Li^+ may be suggested through the systematic decrease of r_{LiD} with increasing LiBr concentration. However, the present r_{LiD} value for the 10 mol% LiBr solution (r_{LiD}=2.71(2) Å) seems too large when compared with the values, r_{LiD}=2.55(2)Å[12] and 2.52(2) Å,[24] reported for 6.7 mol% LiCl heavy water solutions in which the hydration number of Li^+ is reported to be ca. 6. Further, the tilt angle between the $Li^+\cdots O$ axis and the molecular plane of D_2O molecule in the first hydration shell, calculated from the present values of r_{LiO} (=1.98(2) Å) and r_{LiD} (=2.71(2) Å) for 10 mol% LiBr solution, and combining with the intramolecular structure of D_2O in highly concentrated LiCl solutions,[43] results to be 0 °C. This value disagrees with the previous observations.[12,24] Before discussing the concentration dependence of the hydration geometry of the water molecules in the first hydration shell of Li^+ in the present system, it is necessary to consider the effect of the statistical errors in the high-Q region of the observed $\Delta_{Li}(Q)$ because the functional of the present $G_{Li}(r)$ might be affected from the uncertainties in the observed $\Delta_{Li}(Q)$ through the Fourier transformation. Another analytical procedure which is independent of the Fourier transform is therefore needed.

We next attempt the least-squares fitting analysis for $\Delta_{Li}(Q)$ in Q-space, in order to examine the above results obtained from the fit of $G_{Li}(r)$ in the r-space and to obtain structural information concerning the long-range interaction in these solutions. The theoretical interference function, $\Delta_{Li}{}^{calc}(Q)$, can be written as the sum of the short-range ($i_s{}^{calc}(Q)$) and long-range ($i_l{}^{calc}(Q)$) interaction terms as below,[44—46]

$$\begin{aligned}\Delta_{Li}{}^{calc}(Q)&=i_s{}^{calc}(Q)+i_l{}^{calc}(Q)\\&=\sum 2xn_{Lij}(b_{Li}-b'_{Li})b_j\exp(-l_{Lij}{}^2Q^2/2)\sin(Qr_{Lij})/(Qr_{Lij})\\&+4\pi\rho(A+B+C+D)\\&\times\exp(-l_{0Lij}{}^2Q^2/2)[Qr_{0Lij}\cos(Qr_{0Lij})-\sin(Qr_{0Lij})]Q^{-3}. \quad (6)\end{aligned}$$

Contributions from the atomic pairs in the first hydration shell of Li^+, $Li^+\cdots O$, $Li^+\cdots D$, and $Li^+\cdots Br^-$ for 25 and 33 mol% LiBr solutions, $Li^+\cdots O$, $Li^+\cdots D$ for 10 mol% LiBr solution, are involved in $i_s^{calc}(Q)$. Parameters denoting the long-range continuous distribution, l_{0Lij} and r_{0Lij} were assumed to be identical for all $Li^+\cdots X$ (X=O, D, Br, and Li) interactions, which leads to the reduction of the number of independent parameters. The contribution from the second hydration shell, which is evident in the observed $G_{Li}(r)$ for 25 and 33 mol% LiBr solutions, is also included in $i_s^{calc}(Q)$. The second hydration shell of Li^+ can be divided, in principle, into the contributions from $Li^+\cdots O$, $Li^+\cdots D$, and possibly $Li^+\cdots Br^-$ and $Li^+\cdots Li^+$ pairs; however, it seems difficult in the present time to determine reliable structure parameters for individual atomic pairs because of the extremely broadened feature of the second hydration shell in the observed $G_{Li}(r)$. Reliable parameters for the hydration geometry of water molecules in the second hydration shell may be obtained by the knowledge based on the partial distribution functions, $g_{LiO}(r)$ and $g_{LiD}(r)$. This will be a future research subject. Consequently, in the present analysis, the contribution of the second hydration shell is treated as a single interaction, in which the coherent scattering length in Eq. 6, b_j, is assumed to the sum of deuterium and oxygen atoms within a D_2O molecule; $2b_D+b_O$. The coordination number, $n_{Li\cdots D_2O}$, for the second neighbor shell may be regarded as the maximum number of D_2O molecules, since contributions from $Li^+\cdots Br^-$ and probably $Li^+\cdots Li^+$ pairs can be involved in the second coordination shell of Li^+. The fitting range of Q was taken to be $0.32\leq Q\leq 9.69$ Å^{-1} using the SALS program,[41] assuming that the statistical error distributes uniformly over the whole range of Q. In the preliminary analysis of $\Delta_{Li}(Q)$ for 10 mol% LiBr solution, it was found that a significant improvement of the fit in the low-Q region is feasible by introducing the contribution from the second hydration shell, although the second hydration peak is not well-defined in the observed $G_{Li}(r)$. We therefore employed the theoretical $\Delta_{Li}(Q)$, involving the contribution from the second hydration shell of Li^+.

The result of the least-squares fit for observed $\Delta_{Li}(Q)$ is shown in Fig. 4. A satisfactory agreement is obtained at all compositions between observed and calculated $\Delta_{Li}(Q)$ in the whole Q-range. Final values of all independent parameters are summarized in Table 3. The number of water molecules in the first hydration shell reduced from 5.6(2) for 10 mol% LiBr solution to 3.5(2) for 25 and 33 mol% LiBr solutions, confirming the concentration-dependent hydration number of Li^+ found in the r-space fit described above. The coordination numbers for the first nearest neighbor interactions, $Li^+\cdots O$ and $Li^+\cdots Br^-$, from the Q-space fit, exhibit smaller values than those obtained from the r-space fit. The difference in estimation of the overlap with the longer-range contribution seems to be the reason for the difference in these parameters. The contributions from the second neighbor shell and the long-range continuous distribution seem to be properly estimated in the Q-space fit, whereas these longer-range contributions involved in the first coordination shell in the observed $G_{Li}(r)$, are ignored in the r-space fit. Values of the coordination number obtained from the Q-space fit is therefore considered to be more reliable. The coordination number for the nearest neighbor $Li^+\cdots Br^-$ correlation in the 33 mol% LiBr solution is determined to be 2.9(2), implying that each Br^- is shared by ca. 3 Li^+. Additionally, although less definitively, the $Li^+\cdots Br^-$ correlation is identified around r=3.3 Å for 25 mol% LiBr solution. The coordination number, n_{LiBr}=1.2(5), indicates that substan-

Table 3. Results of the Least-Square Refinements for the Observed $\Delta_{Li}(Q)$ in Q-Space[a]

$i\cdots j$		10 mol% LiBr	25 mol% LiBr	33 mol% LiBr
	r_{ij}/Å	1.96(2)	1.95(2)	1.96(2)
$Li^+\cdots O(I)$[b]	l_{ij}/Å	0.12(2)	0.10(2)	0.10(2)
	n_{ij}	5.6(2)	3.5(2)	3.5(2)
	r_{ij}/Å	2.58(2)	2.58(2)	2.56(2)
$Li^+\cdots D(I)$[b]	l_{ij}/Å	0.30(2)	0.21(2)	0.30(1)
	r_{ij}/Å	—	3.3(2)	3.37(2)
$Li^+\cdots Br^-$	l_{ij}/Å	—	0.5(1)	0.14(4)
	n_{ij}	—	1.2(5)	2.9(2)
	r_{ij}/Å	4.0(1)	4.63(2)	5.03(2)
$Li^+\cdots D_2O(II)$[c]	l_{ij}/Å	0.73(2)	0.56(2)	0.55(2)
	n_{ij}	8.2(2)	8.0(3)	12(2)
	r_{0ij}/Å	4.7(1)	5.14(2)	5.79(2)
$Li^+\cdots X$[d]	l_{0ij}/Å	0.53(2)	0.80(5)	0.57(2)

a) Estimated standard deviations are given in parentheses. b) The first nearest neighbor interaction. c) The second nearest neighbor interaction. d) The long-range interaction (X=O, D, Br, and Li).

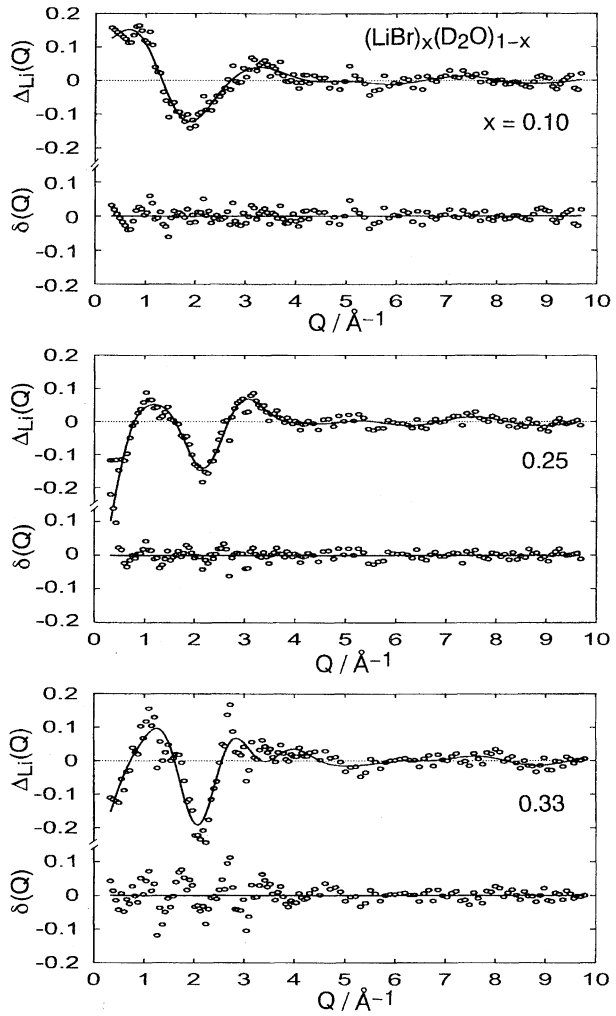

Fig. 4. Observed $\Delta_{Li}(Q)$ for aqueous LiBr solutions, $(LiBr)_x(D_2O)_{1-x}$, x=0.10, 0.25, and 0.33 (circles) and the best fit of the theoretical interference function, $\Delta_{Li}^{calc}(Q)$, defined by Eq. 6 (solid line). The residual function, $\delta(Q)$, is shown below.

tially all the lithium ions form the solvent-shared ion pair in the 25 mol% LiBr solution. On the other hand, the concentration dependence of the hydration geometry of the water molecules in the first hydration shell can not be observed in the results. The values of r_{LiO} (1.96(2) Å) and r_{LiD} (2.58(2) Å) for 10 mol% LiBr solution obtained from the Q-space fit are appreciably reduced compared with those from the r-space fit, and the values are now in good agreement with those reported in previous neutron works.[11—24] The fact may suggest that an apparent intermolecular bond length obtained from the observed $G_{Li}(r)$ might be considerably influenced by the statistical errors in the observed $\Delta_{Li}(Q)$. In order to examine the effect of such statistical uncertainties on the distribution function, the observed $\Delta_{Li}(Q)$ was multiplied by the modification function, $M(Q)$=exp(−0.002 Q^2), and then Fourier transformed to obtain the modified distribution function, $G_{Li}(r)$, which is shown in Fig. 5. In the modified $G_{Li}(r)$, high-frequency periodical ripples which appeared at higher-r region in the unmodified $G_{Li}(r)$ (Fig. 3) are almost suppressed. The fact suggests that the periodical ripples in the unmodified $G_{Li}(r)$ are mainly due to the statistical uncertainties in the observed $\Delta_{Li}(Q)$ in the high-Q region. It may be concluded that the small peakes which appear in the range of $4 \leq r \leq 6$ Å in the unmodified $G_{Li}(r)$ for 33 mol% LiBr solution does not correspond to any real structure. On the other hand, broadened features located at r=5.0 and 7.6 Å in the modified $G_{Li}(r)$ for 33 mol% LiBr solution, are considered to reflect the real ones, indicating that medium-range order may exist in the solution. The solid line Fig. 5 represents the Fourier transform of the theoretical interference function multiplied by $M(Q)$, $M(Q)\cdot\Delta_{Li}^{calc}(Q)$, calculated by using the best-fit parameters listed in Table 3. The agreement between the observed and calculated $G_{Li}(r)$ seems again satisfactory. The first-nearest-neighbor contributions obtained by the Fourier transform of individual $Li^+\cdots O$, $Li^+\cdots D$, and $Li^+\cdots Br^-$ interference functions multiplied by $M(Q)$, are indicated by dotted lines. The intermolecular distance cor-

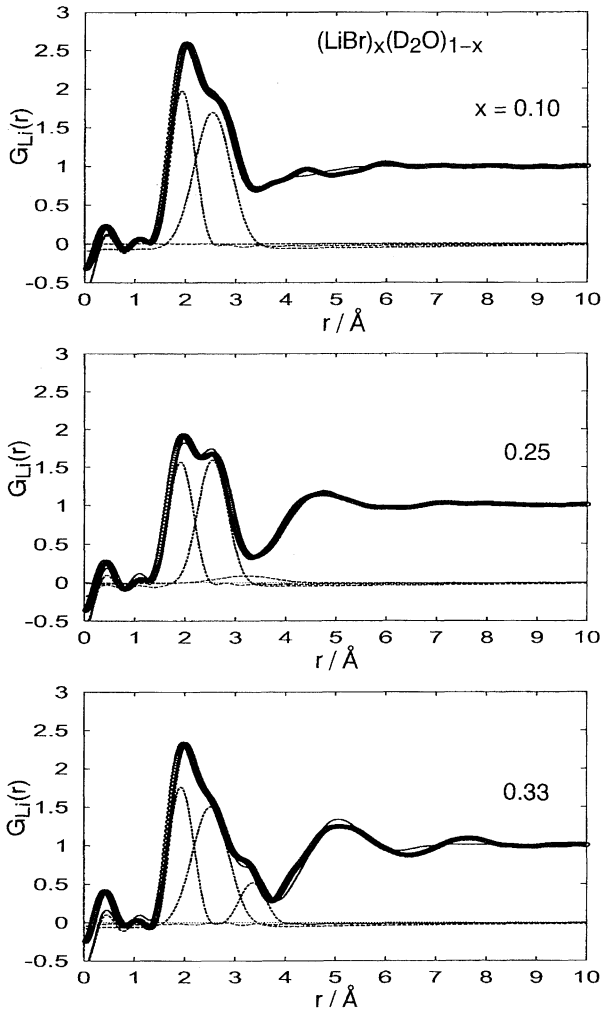

Fig. 5. The modified distribution functions around Li^+, $G_{Li}(r)$ for aqueous LiBr solutions, $(LiBr)_x(D_2O)_{1-x}$, x= 0.10, 0.25, and 0.33 (circles). Solid lines are given by the Fourier transform of the solid lines in Fig. 4. The nearest neighbor contributions from $Li^+\cdots O$, and $Li^+\cdots D$, and $Li^+\cdots Br^-$ pairs are shown by broken lines.

responding to the second hydration shell seems to increase with increasing LiBr concentration; however, in such highly concentrated solutions, the contribution from the $Li^+\cdots Br^-$ as well as $Li^+\cdots Li^+$ interactions should be involved in the second coordination shell of Li^+. Obviously, the structural determination in the partial distribution level is needed for describing the hydration geometry of water molecules in the second coordination shell. Along this line, data analyses of neutron diffraction experiments with H/D isotopic substitution technique for these solutions are now in progress.

The authors would like to express their thanks to The Institute of Solid State Physics (ISSP), University of Tokyo, for providing us to use the diffractometer PANSI in JRR-2. The author are also grateful to Professor Hideki Yoshizawa (University of Tokyo) and Mr.Yoshihisa Kawamura (University of Tokyo) for their help during the course of the diffraction measurement. All of the calculations were carried out with the SUN 4/1000 computer at the Computing Center of Yamagata University. This work was partially supported by a Grant-in-Aid for Scientific Research No. 06640712 from the Ministry of Education, Science and Culture.

References

1) G. W. Brady, *J. Chem. Phys.*, **28**, 464 (1958).
2) R. M. Lawrence and R. F. Kruch, *J. Chem. Phys.*, **47**, 4758 (1967).
3) G. Licheri, G. Piccaluga, and G. Pinna, *J. Appl. Crystallogr.*, **6**, 392 (1973).
4) A. H. Narten, F. Vaslow, and H. A. Levy, *J. Chem. Phys.*, **58**, 5017 (1973).
5) G. Licheri, G. Piccaluga, and G. Pinna, *Chem. Phys. Lett.*, **35**, 119 (1975).
6) T. Radnai, G. Pálinkás, Gy. I. Szász, and K. Heinzinger, *Z. Naturforsch., A*, **36A**, 1076 (1981).
7) I. Okada, Y. Kitsuno, H-G. Lee, and H. Ohtaki, "Ions and Molecules in Solution," ed by N. Tanaka, H. Ohtaki, and R. Tamamushi, in "Studies in Physical and Theoretical Chemistry, Elsevier, Amsterdam (1982), Vol. 27, p. 81.
8) P. Bopp, I. Okada, H. Ohtaki, and K. Heinzinger, *Z. Naturforsch., A*, **40A**, 116 (1985).
9) Y. Tamura, K. Tanaka, E. Spohr, and K. Heinzinger, *Z. Naturforsch., A*, **43A**, 1103 (1988).
10) K. Yamanaka, M. Yamagami, T. Takamuku, T. Yamaguchi, and H. Wakita, *J. Phys. Chem.*, **97**, 10835 (1993).
11) N. Ohtomo and K. Arakawa, *Bull. Chem. Soc. Jpn.*, **52**, 2755 (1979).
12) J. R. Newsome, G. W. Neilson, and J. E. Enderby, *J. Phys. C: Solid State Phys.*, **13**, L923 (1979).
13) J. R. Newsome, Ph. D Thesis, University of Bristol, (1981).
14) T. Yamaguchi, Y. Tamura, I. Okada, H. Ohtaki, M. Misawa, and N. Watanabe, "KENS REPORT-V," (1984), p. 54.
15) K. Ichikawa, Y. Kameda, T. Matsumoto, and M. Misawa, *J. Phys. C: Solid State Phys.*, **17**, L725 (1984).
16) K. Ichikawa, Y. Kameda, T. Matsumoto, M. Misawa, and N. Watanabe, "KENS REPORT-V," (1984), p. 58.
17) T. Yamaguchi, S. Tanaka, H. Wakita, and M. Misawa, "KENS REPORT-VII," (1988), p. 48.
18) J. R. C. van der Maarel, D. H. Powell, A. K. Jawahier, L. H. Leyte-Zuidenweg, G. W. Neilson, and M-C. Bellicent-Funel, *J. Chem. Phys.*, **90**, 6709 (1989).
19) T. Cartailler, W. Kuntz, P. Turq, and M-C. Bellicent-Funel, *J. Phys.: Condens. Matter*, **3**, 9511 (1991).
20) T. Yamaguchi, S. Tanaka, H. Wakita, and M. Misawa, "KENS REPORT-VIII," (1991), p. 90.
21) Y. Kameda and O. Uemura, *Bull. Chem. Soc. Jpn.*, **66**, 384 (1993).
22) M. Yamagami, T. Yamaguchi, H. Wakita, and M. Misawa, *J. Chem. Phys.*, **100**, 3122 (1994).
23) M. Yamagami, H. Wakita, T. Yamaguchi, M. Misawa, and T. Fukunaga, "KENS REPORT-X,"(1995), p. 105.
24) I. Howell and G. W. Neilson, *J. Phys.: Condens. Matter*, **8**, 4455 (1996).
25) H. Ohtaki and T. Radnai, *Chem. Rev.*, **93**, 1157 (1993).
26) A. K. Soper, G. W. Neilson, J. E. Enderby, and R. A. Howe, *J. Phys. C: Solid State Phys.*, **10**, 1793 (1977).
27) J. E. Enderby and G. W. Neilson, "Water, A Comprehensive Treatise," ed by F. Franks, Plenum Press, New York (1979), Vol. 6, p. 1.
28) A. P. Copestake, G. W. Neilson, and J. E. Enderby, *J. Phys. C: Solid State Phys.*, **18**, 4211 (1985).
29) Y. Kameda, H. Ebata, and O. Uemura, *Bull. Chem. Soc. Jpn.*, **67**, 929 (1994).
30) W. Rudolph, W. H. Brooker, and C. C. Pye, *J. Phys. Chem.*, **99**, 3793 (1995).
31) R. H. Tromp, G. W. Neilson, and A. K. Soper, *J. Chem. Phys.*, **96**, 8460 (1992).
32) B. Prével, J. F. Jal, J. Dupuy-Philon, and A. K. Soper, *J. Chem. Phys.*, **103**, 1886 (1995).
33) B. Prével, J. F. Jal, J. Dupuy-Philon, and A. K. Soper, *J. Chem. Phys.*, **103**, 1897 (1995).
34) V. F. Sears, "Thermal-Neutron Scattering Lengths and Cross Sections for Condensed Matter Research," AECL-8490, Atomic Energy of Canada Ltd., (1984), p. 16.
35) J. G. Powles, *Adv. Phys.*, **22**, 1 (1973).
36) J. R. Granada, V. H. Gillete, and R. E. Mayer, *Phys. Rev. A*, **36**, 5594 (1987).
37) H. H. Paalman and C. J. Pings, *J. Appl. Phys.*, **33**, 2635 (1962).
38) I. A. Blech and B. L. Averbach, *Phys. Rev.*, **137**, A1113 (1965).
39) J. G. Powles, *Mol. Phys.*, **26**, 1325 (1973).
40) J. G. Powles, *Mol. Phys.*, **42**, 757 (1981).
41) T. Nakagawa and Y. Oyanagi, "Recent Development in Statistical Inference and Data Analysis," ed by K. Matushita, North-Holland (1980), p. 221.
42) E. Weiss, H. Hensel, and H. Kühr, *Chem. Ber.*, **102**, 632 (1969).
43) K. Ichikawa and Y. Kameda, *J. Phys.: Condens. Matter*, **1**, 257 (1989).
44) A. H. Narten, M. D. Danford, and H. A. Levy, *Discuss. Faraday Soc.*, **43**, 97 (1967).
45) R. Caminiti, P. Cucca, M. Monduzzi, G. Saba, and G. Crisponi, *J. Chem. Phys.*, **81**, 543 (1984).
46) H. Ohtaki and N. Fukushima, *J. Solution Chem.*, **21**, 23 (1992).